

Cancer Cell, Volume 33

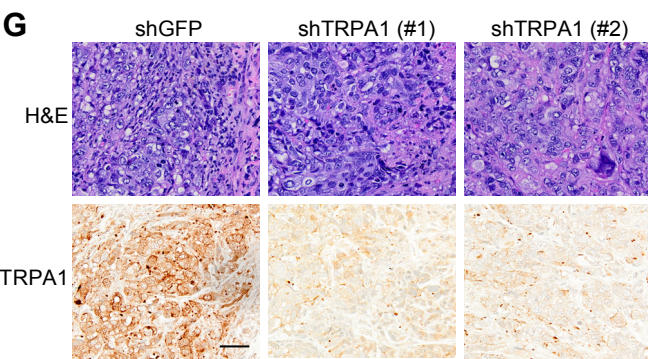
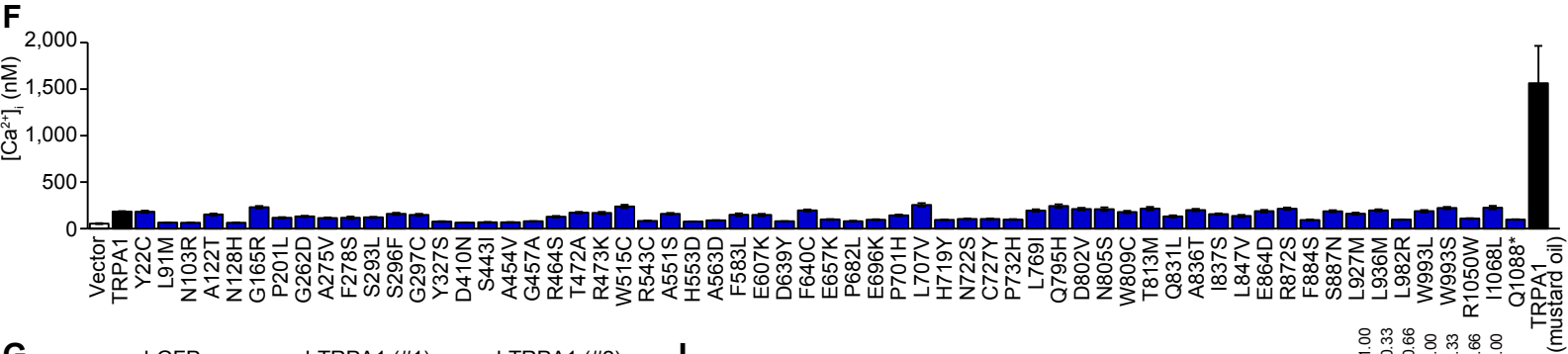
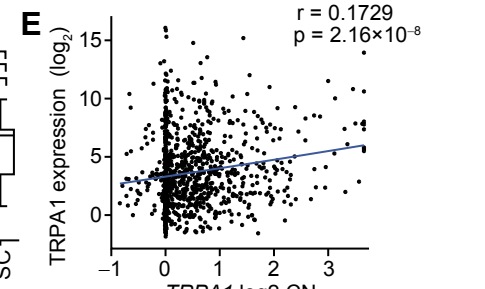
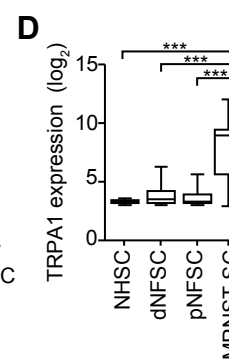
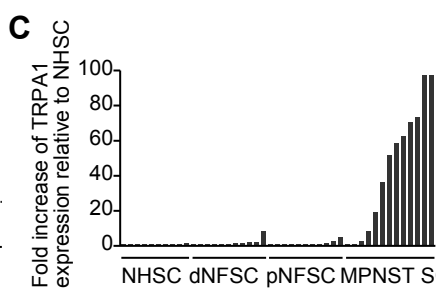
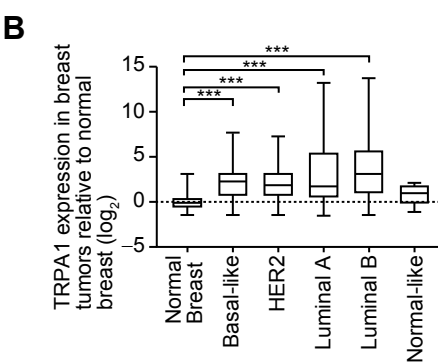
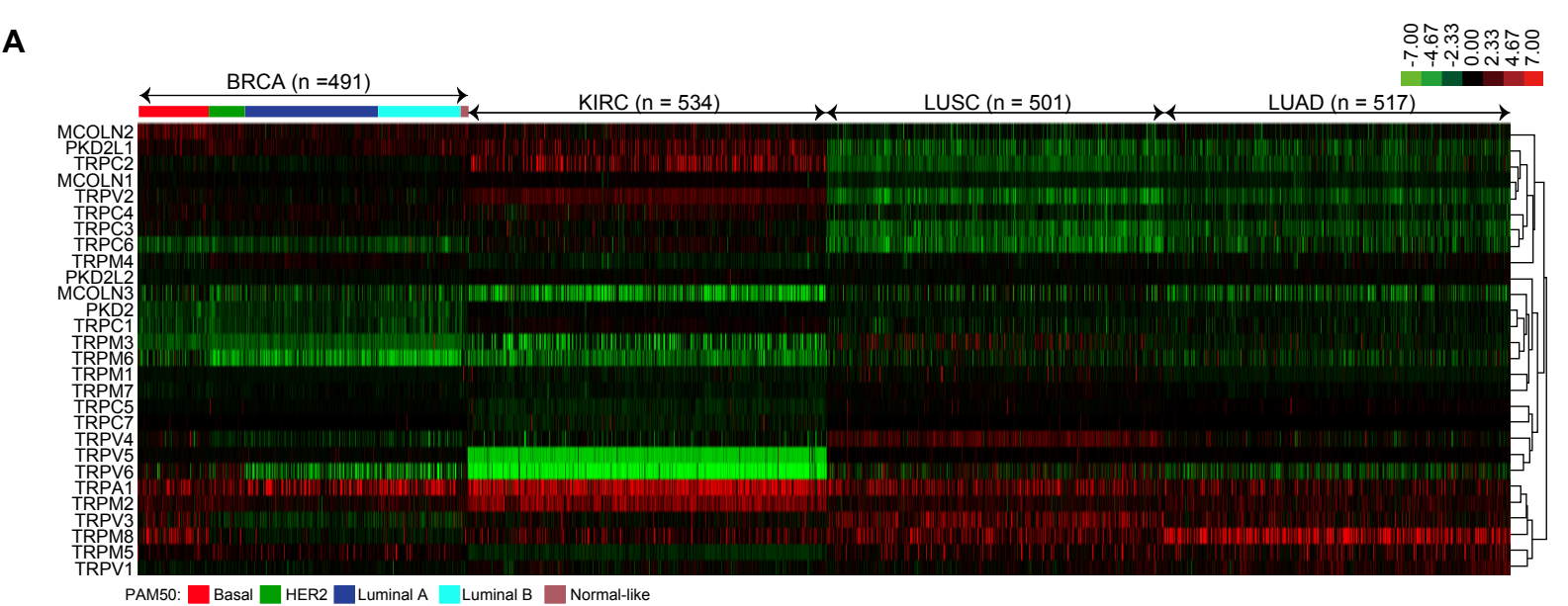
Supplemental Information

Cancer Cells Co-opt

the Neuronal Redox-Sensing Channel TRPA1

to Promote Oxidative-Stress Tolerance

Nobuaki Takahashi, Hsing-Yu Chen, Isaac S. Harris, Daniel G. Stover, Laura M. Selfors, Roderick T. Bronson, Thomas Deraedt, Karen Cichowski, Alana L. Welm, Yasuo Mori, Gordon B. Mills, and Joan S. Brugge



I

PDX model	HCl 001 P3	HCl 001 P7	HCl 002 P3	HCl 002 P7	HCl 003 P3	HCl 003 P6	HCl 004 P3	HCl 005 P3	HCl 006 P3	HCl 007 P3	HCl 008 P4	HCl 009 P3	HCl 009 P6	HCl 010 P3	HCl 011 P3	HCl 011 P4	HCl 012 P4
ER/PR/HER2	-/-	-/-	-/-	-/-	+/+	+/+	-/-	+/+	+/+	+/+	-/-	-/-	-/-	-/-	+/+	+/+	-/-
TRPA1	Green	Green	Black	Black	Red	Red	N.D.	Green	Green	Green	N.D.	N.D.	N.D.	Green	Red	Red	Green

N.D.: Not detected

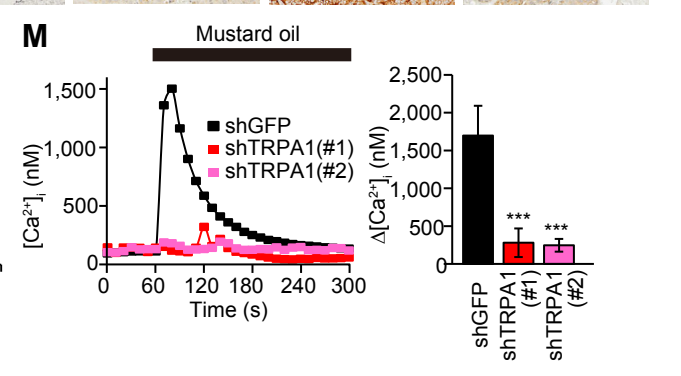
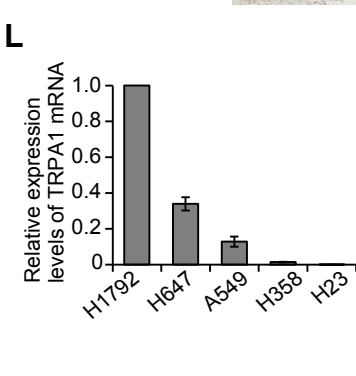
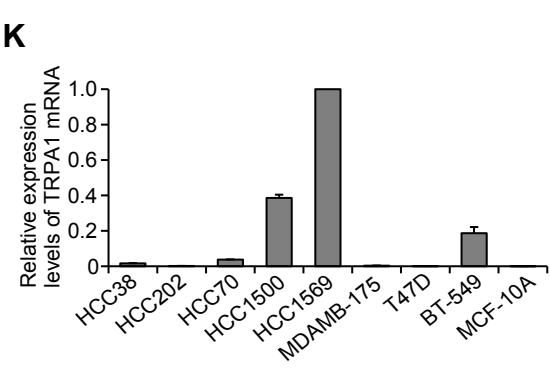
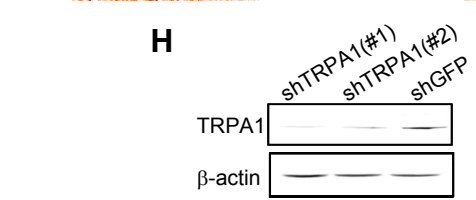
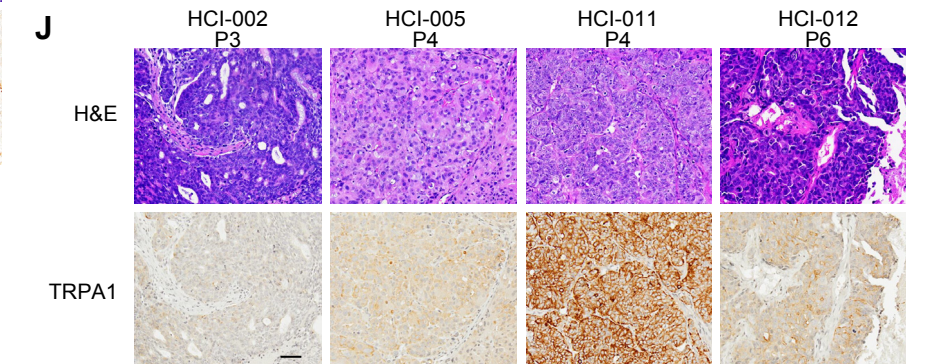


Figure S1. TRPA1 Is Upregulated in Diverse Tumor Types, Related to Figure 1.

(A) Heatmap (red, increased expression; green, decreased expression) of TRP channel mRNA levels in TCGA BRCA, KIRC, LUSC, and LUAD relative to corresponding normal tissues (n = 121 for BRCA, n = 72 for KIRC, n = 51 for LUSC, and n = 59 for LUAD). The samples, whose PAM50 has not been identified, are not included for BRCA. Averaged mRNA level of each TRP channel relative to corresponding normal tissues are listed in Table S1.

(B) Box plots displaying TRPA1 mRNA levels in Basal-like (n = 107), HER2 (n = 51), Luminal A (n = 201), Luminal B (n = 123), and Normal-like (n = 9) subtypes of BRCA relative to normal breast tissues (n = 121). ***p < 0.001 (one-way ANOVA).

(C) Waterfall plot displaying fold increases of TRPA1 mRNA expression in dermal and plexiform NF1-derived primary benign neurofibroma Schwann (dNFSCs and pNFSCs, respectively) and MPNST Schwann cells (MPNST SC) relative to normal human Schwann cells (NHSC), using a published microarray dataset (Miller et al., 2009). The vertical axis of the graph is cut off at 100.

(D) Box plots displaying TRPA1 mRNA levels in NHSC (n = 10), dNFSC (n = 11), pNFSC (n = 11), and MPNST SC (n = 13). ***p < 0.001 (one-way ANOVA).

(E) Correlation of *TRPA1* copy number (CN) alterations with TRPA1 mRNA expression in BRCA (n = 1036).

(F) Averaged intracellular Ca²⁺ concentration ([Ca²⁺]_i) upon treatment with or without 30 μM mustard oil in HEK293 cells transfected with TRPA1 mutant construct. Data shown as mean ± SEM (n = 37–208). Cancer types where each mutation was found are listed in Table S2.

(G) Representative H&E (upper panels) and TRPA1 IHC staining (lower panels) of the indicated HCC1569 xenograft tumor sections from three independent experiments. TRPA1 antibody from Sigma. Scale bar 50 μm.

(H) Immunoblot analysis of TRPA1 in HCC1569 cells transduced with shRNA against TRPA1 or GFP (control) from two independent experiments. TRPA1 antibody from Novus.

(I) Heatmap representing relative levels of TRPA1 mRNA in PDX models (DeRose et al., 2011). The data are expressed as log₂ median-centered ratio. P represents passage number.

(J) H&E (upper panels) and TRPA1 IHC staining (lower panels) of the indicated PDX tumor sections. Scale bar 50 μm.

(K) TRPA1 mRNA levels in the indicated breast cancer cell lines as determined by quantitative PCR. Data are normalized to HCC1569 cells. Data shown as the mean ± SEM of three independent experiments.

(L) TRPA1 mRNA levels in the indicated lung cancer cell lines as determined by quantitative PCR. Data are normalized to H1792 cells. Data shown as the mean ± SEM of three independent experiments.

(M) Averaged time courses and the maximal [Ca²⁺]_i rises (Δ[Ca²⁺]_i) evoked by 30 μM mustard oil in HCC1569 cells transduced with shTRPA1 or shGFP. Data shown as mean ± SEM (n = 9–59). ***p < 0.001 compared to shGFP (Student's t test).

In (B) and (D), box and whiskers graphs indicate the median and the 25th and 75th percentiles, with minimum and maximum values at the extremes of the whiskers.

Table S1. Averaged TRP channel mRNA levels in TCGA BRCA, KIRC, LUSC, and LUAD relative to corresponding normal tissues (n = 121 for BRCA, n = 72 for KIRC, n = 51 for LUSC, and n = 59 for LUAD), related to Figure 1.

BRCA (n = 491)					KIRC (n = 534)				
Ranking	TRP subtype	mRNA level relative to normal breast tissues (log ₂)	p value (vs normal breast)	p value (vs TRPA1)	Ranking	TRP subtype	mRNA level relative to normal kidney tissues (log ₂)	p value (vs normal lung)	p value (vs TRPA1)
1	*TRPA1	2.87	5.03×10⁻²²		1	*TRPA1	4.18	1.19×10⁻⁵¹	
2	MCOLN2	1.23	4.87×10 ⁻²⁰	2.23×10 ⁻²⁷	2	*TRPM2	3.15	4.96×10 ⁻⁷⁶	1.78×10 ⁻²⁴
3	PKD2L1	1.17	1.26×10 ⁻¹³	4.71×10 ⁻³¹	3	*TRPV2	2.13	4.31×10 ⁻⁸⁰	3.27×10 ⁻⁹²
4	*TRPM2	1.10	1.39×10 ⁻¹⁹	2.57×10 ⁻³²	4	TRPC2	2.13	2.65×10 ⁻¹²	1.38×10 ⁻⁴⁸
5	TRPM5	0.924	6.53×10 ⁻⁹	1.72×10 ⁻³⁷	5	PKD2L1	1.62	3.47×10 ⁻¹⁶	1.07×10 ⁻⁹⁸
6	TRPC4	0.505	4.19×10 ⁻⁷	1.16×10 ⁻⁵⁵	6	TRPM8	1.27	5.77×10 ⁻⁶	1.00×10 ⁻¹¹³
7	TRPM4	0.310	2.22×10 ⁻⁶	2.50×10 ⁻⁶³	7	TRPC4	0.841	2.03×10 ⁻⁷	4.15×10 ⁻¹⁶⁵
8	TRPM8	0.102	0.758	3.15×10 ⁻⁵⁵	8	MCOLN2	0.644	1.39×10 ⁻⁵	1.46×10 ⁻¹⁷⁶
9	TRPC7	0.0581	0.0892	1.13×10 ⁻⁷⁹	9	TRPC1	0.515	3.38×10 ⁻¹⁰	4.44×10 ⁻²¹⁹
10	MCOLN1	0.0269	0.895	1.07×10 ⁻⁷⁹	10	TRPC6	0.458	0.000599	1.06×10 ⁻¹⁹³
11	*TRPV2	0.0103	0.788	4.39×10 ⁻⁷⁶	11	MCOLN1	0.342	1.81×10 ⁻⁹	2.36×10 ⁻²⁴¹
12	TRPV5	-0.0186	0.0198	1.63×10 ⁻⁸⁰	12	PKD2L2	0.181	0.0443	1.72×10 ⁻²⁴⁵
13	TRPC3	-0.0945	0.721	2.08×10 ⁻⁸⁰	13	*TRPV1	0.154	0.0223	2.78×10 ⁻²²¹
14	*TRPC5	-0.269	6.74×10 ⁻¹²	2.96×10 ⁻⁹⁴	14	*TRPV3	0.116	0.346	3.74×10 ⁻²¹⁴
15	*TRPV1	-0.330	2.18×10 ⁻⁵	1.95×10 ⁻⁹³	15	PKD2	-0.114	0.000892	5.16×10 ⁻²⁷²
16	PKD2L2	-0.404	2.65×10 ⁻¹⁰	1.66×10 ⁻⁹⁹	16	TRPC3	-0.200	0.302	1.83×10 ⁻²⁴⁹
17	TRPC2	-0.448	1.49×10 ⁻⁶	2.18×10 ⁻⁹⁸	17	*TRPV4	-0.534	0.00209	2.86×10 ⁻²⁵⁸
18	*TRPM7	-0.456	2.33×10 ⁻⁹	1.35×10 ⁻¹⁰¹	18	TRPM1	-0.683	4.64×10 ⁻⁹	1.24×10 ⁻²⁹¹
19	*TRPV3	-0.577	0.00621	7.96×10 ⁻⁸⁷	19	*TRPM7	-0.743	3.14×10 ⁻²³	0
20	TRPM1	-0.628	1.11×10 ⁻³⁴	4.41×10 ⁻¹¹¹	20	TRPC7	-0.858	2.09×10 ⁻¹²	5.99×10 ⁻²⁹¹
21	*TRPV4	-0.773	0.00496	5.21×10 ⁻¹⁰⁶	21	TRPM4	-0.936	4.38×10 ⁻²²	0
22	MCOLN3	-1.23	1.00×10 ⁻¹²	1.58×10 ⁻¹¹⁴	22	*TRPC5	-1.20	1.64×10 ⁻²⁹	0
23	TRPV6	-1.56	0.00710	3.32×10 ⁻¹⁰³	23	TRPM5	-1.37	1.94×10 ⁻⁵⁸	0
24	TRPC1	-1.59	1.12×10 ⁻⁴⁸	2.88×10 ⁻¹⁵⁰	24	TRPM3	-2.41	1.96×10 ⁻¹⁵	1.10×10 ⁻²⁸⁹
25	PKD2	-1.69	1.11×10 ⁻⁷¹	8.06×10 ⁻¹⁵⁹	25	TRPM6	-2.82	1.30×10 ⁻⁴⁰	0
26	TRPC6	-1.87	1.09×10 ⁻⁵⁷	2.19×10 ⁻¹⁶³	26	MCOLN3	-3.30	8.53×10 ⁻³⁵	0
27	TRPM3	-2.55	4.16×10 ⁻¹¹⁷	7.71×10 ⁻²⁰¹	27	TRPV5	-4.76	4.85×10 ⁻¹³³	0
28	TRPM6	-3.06	1.68×10 ⁻⁵³	1.62×10 ⁻¹⁹²	28	TRPV6	-6.18	5.63×10 ⁻¹⁵⁸	0

LUSC (n = 501)					LUAD (n = 517)				
Ranking	TRP subtype	mRNA level relative to normal lung tissues (log ₂)	p value (vs normal lung)	p value (vs TRPA1)	Ranking	TRP subtype	mRNA level relative to normal lung tissues (log ₂)	p value (vs normal lung)	p value (vs TRPA1)
1	*TRPA1	2.27	1.25×10⁻¹³		1	TRPM8	3.90	1.54×10 ⁻²²	1.69×10 ⁻⁶²
2	*TRPV3	2.07	2.99×10 ⁻¹⁴	0.106	2	*TRPA1	1.27	9.08×10⁻⁶	
3	TRPM8	2.01	5.31×10 ⁻¹⁴	0.0380	3	*TRPM2	1.20	1.19×10 ⁻¹⁴	0.49
4	*TRPV4	1.93	7.33×10 ⁻²³	0.00249	4	*TRPV1	1.07	5.82×10 ⁻¹⁶	0.0359
5	*TRPM2	1.09	1.28×10 ⁻²⁰	2.05×10 ⁻²⁶	5	TRPM5	1.05	3.44×10 ⁻⁵	0.0554
6	TRPM5	0.96	0.00212	2.35×10 ⁻²⁴	6	*TRPV3	0.891	1.27×10 ⁻⁶	0.000385
7	*TRPV1	0.37	0.0192	2.61×10 ⁻⁶¹	7	*TRPC5	0.325	0.465	2.54×10 ⁻²⁷
8	TRPV5	0.272	0.138	4.46×10 ⁻⁷⁶	8	TRPV5	0.184	0.404	1.40×10 ⁻³⁶
9	*TRPM7	0.243	0.00302	3.36×10 ⁻⁷⁶	9	*TRPV4	0.0781	0.562	1.01×10 ⁻³⁰
10	TRPC7	0.101	0.0643	1.51×10 ⁻⁸⁸	10	TRPC7	0.0195	0.197	2.23×10 ⁻⁴⁸
11	*TRPC5	0.0929	0.655	4.09×10 ⁻⁸⁵	11	PKD2L2	-0.0170	0.425	1.21×10 ⁻⁴⁶
12	TRPV6	0.0498	0.513	2.70×10 ⁻⁵⁴	12	TRPM4	-0.0950	0.912	3.35×10 ⁻⁴⁴
13	TRPM3	-0.0600	0.896	9.21×10 ⁻⁶²	13	*TRPM7	-0.228	0.00336	3.15×10 ⁻⁶²
14	TRPM1	-0.128	0.0220	7.27×10 ⁻⁸⁴	14	MCOLN2	-0.379	0.0375	1.28×10 ⁻⁵⁶
15	PKD2L2	-0.207	0.0245	9.80×10 ⁻¹⁰⁷	15	TRPC1	-0.608	0.000134	2.97×10 ⁻⁷⁷
16	TRPM4	-0.282	0.135	8.33×10 ⁻¹⁰⁴	16	TRPM3	-0.742	1.17×10 ⁻⁶	3.64×10 ⁻⁸³
17	MCOLN3	-0.635	0.0471	1.53×10 ⁻⁹³	17	PKD2	-0.790	7.06×10 ⁻¹³	1.19×10 ⁻⁹⁹
18	TRPC1	-0.705	6.79×10 ⁻⁵	2.24×10 ⁻¹²⁰	18	TRPM1	-0.821	1.86×10 ⁻²³	6.83×10 ⁻¹⁰⁴
19	TRPM6	-0.721	0.000210	4.65×10 ⁻¹¹⁰	19	MCOLN1	-0.956	1.97×10 ⁻³¹	2.22×10 ⁻¹¹⁷
20	PKD2	-0.772	7.38×10 ⁻²¹	3.32×10 ⁻¹⁴⁴	20	TRPC4	-0.986	1.06×10 ⁻¹²	1.27×10 ⁻¹⁰⁴
21	MCOLN2	-0.798	4.80×10 ⁻⁵	5.53×10 ⁻¹²⁴	21	TRPV6	-1.04	2.32×10 ⁻⁵	3.60×10 ⁻⁶⁹
22	TRPC4	-1.00	2.78×10 ⁻⁹	9.68×10 ⁻¹⁴⁰	22	TRPM6	-1.09	9.44×10 ⁻⁸	1.94×10 ⁻⁹⁰
23	MCOLN1	-1.11	7.12×10 ⁻⁴⁰	2.55×10 ⁻¹⁶⁹	23	TRPC6	-1.40	9.71×10 ⁻¹¹	4.62×10 ⁻¹⁰⁹
24	PKD2L1	-2.12	2.54×10 ⁻¹⁷	2.64×10 ⁻¹⁹²	24	TRPC2	-1.48	1.33×10 ⁻¹⁵	1.09×10 ⁻¹²⁵
25	TRPC2	-2.29	1.57×10 ⁻⁵⁹	4.56×10 ⁻²³⁵	25	PKD2L1	-1.54	2.08×10 ⁻¹³	2.22×10 ⁻¹²³
26	TRPC3	-2.50	4.24×10 ⁻⁴⁸	2.36×10 ⁻²³⁷	26	MCOLN3	-1.68	2.55×10 ⁻¹⁰	1.19×10 ⁻¹¹²
27	TRPC6	-2.67	4.36×10 ⁻⁴⁰	5.59×10 ⁻²³⁵	27	TRPC3	-1.88	5.57×10 ⁻²⁴	8.20×10 ⁻¹⁶²
28	*TRPV2	-2.67	7.90×10 ⁻⁵⁶	4.75×10 ⁻²⁴⁷	28	*TRPV2	-1.97	3.44×10 ⁻⁴⁷	7.00×10 ⁻¹⁸¹

Asterisk (*) denotes redox-sensitive TRP channels

Table S2. Primer sequences used for the construction of TRPA1 mutants, related to Figure 1.

Mutants	Cancer types	Mutation primer sequence (5' → 3')	
		Forward primer	Reverse primer
Y22C	LUSC	agggcgtgttctGtgaggatgtgcc	ggcacatcctcacagaCaacgccct
L91M	Colorectal	cctcttggaaagtAtgcatgaaatggatg	catccatttcatgcaTcacttccaagagg
H103R	Stomach	gaaatacccctctgcGttgtgctgtagaaa	tttctacagcacaacGcagaggggtatttc
A122T	Uterine	ttctcagcagaggaAcaaaccacaacctcc	ggaggtttgggttgTtccctctgctgagaa
N128H	Melanoma	acccaaaccctccgaCacttcaacatgatg	catcatgttgaagtGtcggaggtttgggt
G165R	LUSC	tggaggagaaaaatCgaaacacagctgtga	tcacagctgtgttcGattttcctcca
P201L	Melanoma	aatggggatgttccTtattaccaagctg	cagcttgggaataAggaacatccccatt
G262D	Uterine	tgtcctggacaatgAtgcacaatagacc	ggctattttgtgcaTcattgtccaggcaca
A275V	GBM	agggaaggtgcacagTcattcattttgctg	cagcaaatgaatgActgtgcaccttccct
F278S	Ovarian	cagccattcattCtgcctgccacca	tgggtggcagcaGaatgaatggctg
S293L	Colorectal	gttaaactgatgataTgtcctattctggtagcgtg	cagcctaccagaataggacAataatcagtttaac
S296F	BRCA	gttaaactgatgatactgctctattTtgtagcgtg	cacgctaccaAaataggacgataatcagtttaac
G297C	LUAD	gatatcgtctattctTgtagcgtggatattgt	aacaatatccacgctacAagaataggacgatac
Y327S	Ovarian	catgagctagcagactCtitaattcagtgggag	ctcccactgaaataaaGagctgctagctcatg
D410N	Colorecta & Glioma	tggtaatggatgaaAacaacagatgggtgta	tacaccctcgtgtTttcatccattacca
S443I	Colorectal	cattccaaaATCaaagataagaaatcacctctgc	gcagagggtattcttattGATttggaatg
A454V	Stomach	gcattttgcaGTCagttatggcgatcaa	tgatagcggcacaactGACtgcaaatgc
G457A	LUAD	gcagccagttatGCgctatcaataccctgt	acaggtattgatacGCgataactggctgc
R464S	LUSC	caatacctgtcagAGCctctacaagacataagtg	cacttatgtcttggaggGCTctgacaggtattg
T472A	Stomach	gacataagtgatGCgaggtctgaaatggaag	ccttcattcagaagcctCGCatacattatgc
R473K	Uterine	gacataagtgatagAACcttgaatgaagtgac	gtcaccttcattcagaagCTTcgtatcacttatgc
W515C	LUAD	accacaatggcTGCacagcittgcat	atgcaaatgctGCAGccattgtggt
R543C	Melanoma	tgaagtgcacagatTGCttggatgaagcgc	cgtctcatccaaGCaatctgacacttca
A551S	Colorectal	aagacgggaactTCActtcaactttgctgc	gcagcaaatgaagTGAagttcccgctctt
H553D	LUSC	ggaacactgcactGACttgtctgcaagg	ccttgcagcaaaaGTCaagtgcaagttcc
A563D	LUSC	ccacgcaaaaGACgttgccttctt	aagaagcgaacGTCtttggcgtgg
F583L	Stomach	agcagccctccCTTttgcacctg	gcaaggtgcaaAAGggaggcctgct
E607K	Melanoma	caggagcaaaagatgggatAAAtgtcttaagatttc	gaaaatctaagacaTTTatcccatcttggctcctg
D639Y	Uterine	gcatgaaggtactttatTATtctgcatgtgcatc	gaatgcaacatgcagaaATAaaaagttacattcgc
F640C	Uterine	atgaaggtacttttagatTGCtgcattgtgcatc	gaatgcaacatgcAGCAatcaaaaagttacattc
E657K	Colorectal	gacaagctctgcccagactattatataAGTataattc	gaaatataCTTgatataatgctcggcaggactgtc
P682L	Colorectal	caggatgttatatagaaCTGcttacagccctcaacg	cgttgaggcgtgtaagCAGttcatataaacatcctg
E696K	Melanoma	caaaaataaccgcataAAGcttcaatcatcctg	caggatgattgagaagCTTatgcccgttatttg
P701H	Stomach & Uterine	cgcatagagcttcaatcatCATgtgtgtaagaata	tattctttacacacATGatgattgagaagctatgcg
L707V	Uterine	gtgtgtaagaatatCTActatgaaatgggtggc	gccaaaccattcatgagTAGatattcttacacac
H719Y	LUAD	ggcttatggattagagctTATatgatgaatttaggatc	gatcctaattcatcatATAagctctaaatcataagcc
N722S	LUSC	gagctcatatgatgAGTtaggatcttactgtctgg	ccaagcagtaagatcctaaACTcatcatatgagctc
C727Y	Uterine	gaatttaggatcttacTATcttggctcatacctatgacc	ggcataggtatgagaccaagATAgtaagatcctaattc
P732H	Uterine	gtcttggctcataCATatgaccattctggttgc	gacaacgagaaggtgcatATGtatgacccaagac
L769I	Uterine	ctagataaccagaattcatalATAataaaaactgtatg	catacaagttttatTATatataaactggttatctag
Q795H	Uterine	cggggcaaaatttccaaCACaaaaggaattatt	aataattccttttGTGttgaaaatttgcctccg
D802V	LUAD	ggaattattttatgGTTataagcaatgttctgaaatg	ccattcaagaacattgcttatAACcataaaaataattc
N805S	LUAD	tatggatataagcAGTgttctgaaatgattatctcac	gtgtagataatcattcaagaacACTGcttatatccata
W809C	GBM	atataagcaatgttcttgaaTGCattatctacacgacg	cgtcgtgtagataatGCAttcaagaacattgcttat
T813M	GBM	gaatggattatctacATGacgggcatcattttgt	acaaaatgatgcccgCATgtagataatccattc
Q831L	GBM	agctcatctgCTGtggcaatgtgga	tccacattgccaCAGcagatgagct
A836T	LUAD & Pancreas	tggcaatgtggaACaattgctgttacttct	agaagtaaacagcaatGTtccacattgcca
I837S	Colorectal	tggcaatgtggaACaattgctgttacttct	agaagtaaacagcACTgtctccacattgcca
L847V	Uterine	cttctattggatgaattcGTAttgtatctcaagatt	aatctttgagatataaTACGaaattcatccaatgaga
E864D	Uterine	ggaattttattggtatgtgGACgtaattttgaaac	gltttcaaaattacGTCcaacataacaataaaaattcc
R872S	Glioma	tgaaaacttggtagcTctacagttgattatcttcc	ggaagataaatacaactgtagaGCTcaacaagttttca
F884S	Stomach	ccttctctggctTCTggactcagcttttaca	tgtaaaagctgagtcAGAagccagaagaagg
S887N	Colorectal	ttctggctttggactAACttttacatctcct	aggaggatgtaaaaGTTgagttcaaaagccagaa
L927M	Uterine & Colorectal	tctagaaccatataTGagaatgaattggcac	gtgccaaattcattctCATatattggtctagga
L936M	Colorectal	ggcacatccagttATGtctttgcacaac	gttgtgcaagggaCATaactggatgtgccc
L982R	Stomach	ctatgcaggtggaacCGTcataccagctta	taagctggtatgACGttccacctgcatag
W993L	GBM & NSCLC	gaagctgcccactTTGtttctacgcaaaagt	actttgcgtagaaaCAaaagtggcagcttc
W993S	LUSC	gaagctgcccactTCGtttctacgcaaaagt	actttgcgtagaaaCAaaagtggcagcttc
R1050W	Uterine	taagcagaataacTGGctgaaagatcttactttc	gaaaagtaagatcctcagCCAGtatgttctgcttta
I1068L	LUAD	gagctcattaaactgCTCattcagaagatgg	ccatcttctgaatGAGcagtttaagatgctc
Q1088*	LUSC	gccattgtcttttTAAGacaggttaagaaagacg	gctctttctaaacctgtcTTAaaaagaacaatggc

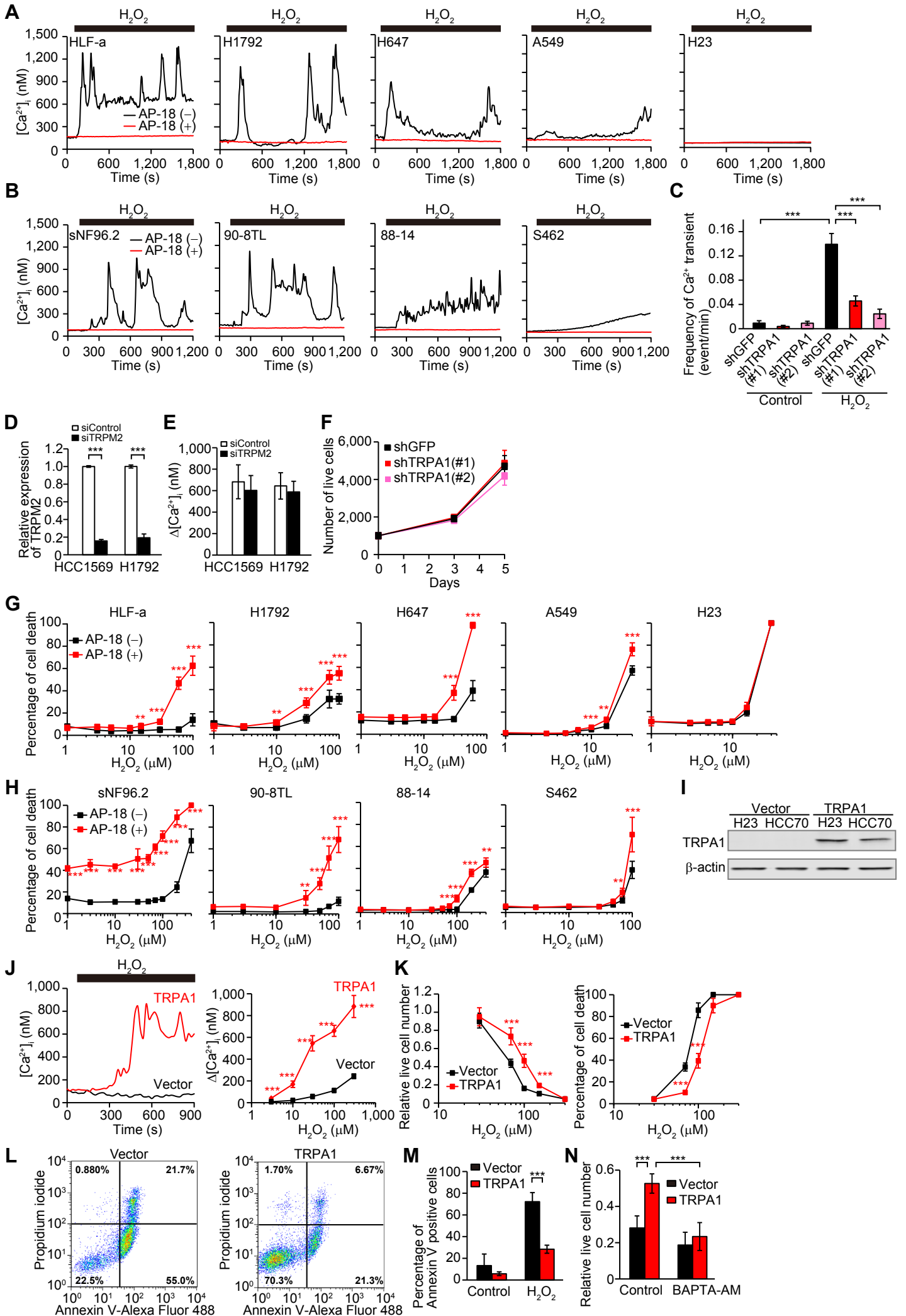


Figure S2. Ca²⁺ Influx through TRPA1 Suppresses Cell Death under Oxidative Stress, Related to Figure 2.

(A and B) Representative time courses of [Ca²⁺]_i changes in the indicated lung cancer (A) or MPNST cells (B) upon treatment with 10 μM H₂O₂ (A) or 30 μM H₂O₂ (B) in the presence or absence of 10 μM AP-18.

(C) Frequency of Ca²⁺ transient (Δ [Ca²⁺]_i > 200 nM) in HCC1569 cells transduced with shTRPA1 or shGFP and treated with or without 10 μM H₂O₂. Data shown as mean ± SEM (n = 35–150). ***p < 0.001 (one-way ANOVA).

(D) mRNA expression of TRPM2 in HCC1569 and H1792 cells transfected with siControl or siTRPM2. Data were normalized to siControl cells. Data shown as mean ± SD of three independent experiments. ***p < 0.001 (Student' s t test).

(E) Δ [Ca²⁺]_i evoked by 10 μM H₂O₂ in the indicated cell lines. Data shown as mean ± SEM (n = 28–34).

(F) Live cell numbers in HCC1569 cells transduced with shTRPA1 or shGFP for the indicated times. Data shown as mean ± SD from the sum of three independent experiments performed in duplicate.

(G and H) Percentage of cell death in the indicated lung cancer (G) and MPNST cells (H) upon treatment with H₂O₂ for 72 hr in the presence or absence of 10 μM AP-18. Data shown as mean ± SD from the sum of three independent experiments performed in duplicate. **p < 0.01 and ***p < 0.001 compared to vehicle control for AP-18 [AP-18 (-)] (Student' s t test).

(I) Immunoblot of lysates from H23 or HCC70 cells transduced with an empty lentiviral vector or TRPA1 from two independent experiments.

(J) Representative time course of [Ca²⁺]_i rises evoked by 100 μM H₂O₂ and dose-response of Δ [Ca²⁺]_i elicited upon treatment with increasing concentrations of H₂O₂ in MCF-10A cells transduced with an empty lentiviral vector or TRPA1. Data shown as mean ± SEM (n = 58–167). ***p < 0.001 compared to vector (Student' s t test).

(K) Live cell numbers relative to H₂O₂-untreated cells and percentage of cell death in the indicated MCF-10A cells upon treatment with H₂O₂ for 72 hr in EGF-free conditions. Data shown as mean ± SD from the sum of three independent experiments performed in duplicate. ***p < 0.001 compared to vector (Student' s t test).

(L) Representative flow cytometric plots of the indicated MCF-10A cells treated with 70 μM H₂O₂ for 72 hr.

(M) Percentage of annexin V-positive cells from experiment in (L). Data shown as mean ± SD of three independent experiments. ***p < 0.001 (Student' s t test).

(N) Live cell numbers relative to H₂O₂-untreated cells in the indicated MCF-10A cells treated with 100 μM H₂O₂ in the presence or absence of 10 μM BAPTA-AM. Data shown as mean ± SD from the sum of two independent experiments performed in triplicate. ***p < 0.001 (one-way ANOVA).

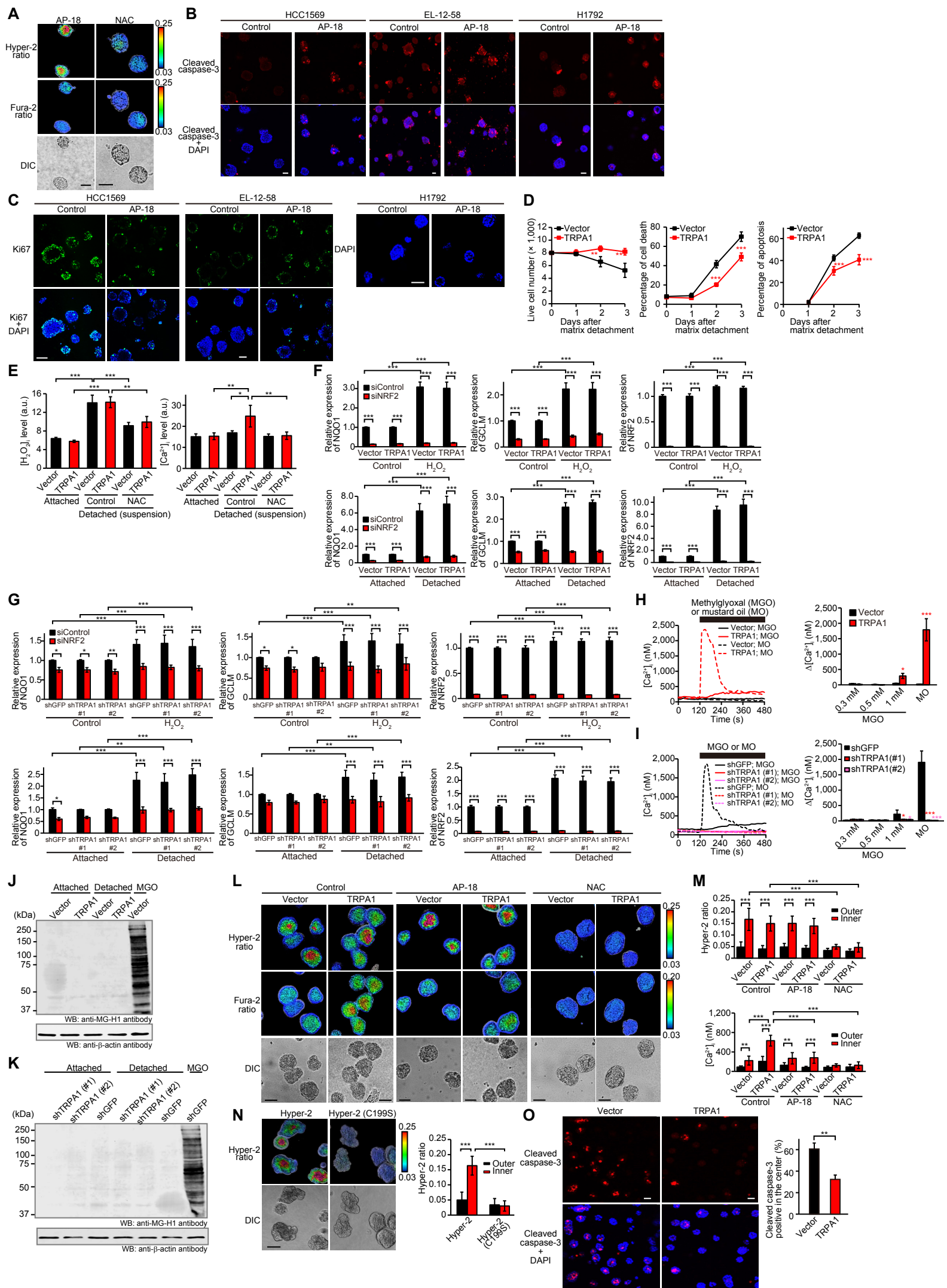


Figure S3. TRPA1 Induces Ca²⁺ Influx in Response to ROS Produced upon Matrix Dissociation and Suppresses Anoikis, Related to Figure 3.

(A) Representative Hyper-2 and fura-2 ratio images of day-5 HCC1569 spheroids transduced with shGFP upon treatment with 10 μ M AP-18 or 5 mM NAC (pH was adjusted to 7.4). Scale bar 50 μ m.

(B) Representative images of day-10 HCC1569, day-10 EL-12-58, or day-6 H1792 spheroids treated with or without 10 μ M AP-18. The spheroids were stained with cleaved caspase-3 and DAPI. Scale bar 50 μ m.

(C) Representative images of day-15 HCC1569, day-15 EL-12-58, or day-10 H1792 spheroids treated with or without 10 μ M AP-18. The spheroids were stained with Ki67 and/or DAPI. Scale bar 100 μ m.

(D) Live cell number, percentage of cell death, and percentage of apoptosis in the indicated MCF-10A cells after matrix detachment for the indicated time. Data shown as mean \pm SD of four independent experiments. ** $p < 0.01$ and *** $p < 0.001$ compared to vector (Student's t test).

(E) Intracellular H₂O₂ and Ca²⁺ levels as determined by peroxy green-1 and Fluo-4 staining, respectively, in MCF-10A cells with an empty lentiviral vector or TRPA1 24 hr after plating in adherent or non-adherent plates. Cells were treated with or without 1 mM NAC. Data shown as mean \pm SD of three independent experiments. * $p < 0.05$, ** $p < 0.01$, and *** $p < 0.001$ (one-way ANOVA).

(F and G) mRNA expression of NQO1, GCLM, or NRF2 in the indicated MCF-10A (F) or HCC1569 cells (G) treated with or without 20 μ M H₂O₂ or cultured in adherent (attached) or non-adherent plates (detached) for 24 hr. Data were normalized to siControl cells treated with vehicle control for H₂O₂. Data shown as mean \pm SD of four independent experiments. * $p < 0.05$, ** $p < 0.01$, and *** $p < 0.001$ (one-way ANOVA).

(H and I) Representative time courses of [Ca²⁺]_i rises evoked by 1 mM methylglyoxal (MGO) or 30 μ M mustard oil (MO), dose-response of Δ [Ca²⁺]_i elicited upon treatment with increasing concentrations of MGO, and Δ [Ca²⁺]_i evoked by 30 μ M MO in the indicated MCF-10A (H) or HCC1569 cells (I). Data shown as mean \pm SEM (n = 8–39). * $p < 0.05$ and *** $p < 0.001$ compared to vector in (H) or shGFP in (I) (Student's t test).

(J and K) Methylglyoxal adducts detected by immunoblotting using anti-MG-H1 antibody in the indicated MCF-10A (J) or HCC1569 cells (K) 24 hr after plating in adherent (attached) or non-adherent plates (detached) or treated with 1 mM MGO for 12 hr. Data from two independent experiments.

(L) Representative Hyper-2 and fura-2 ratio images of day-6 MCF-10A acini transduced with vector or TRPA1 and treated with 10 μ M AP-18 or 5 mM NAC (pH was adjusted to 7.4). Scale bar 50 μ m.

(M) Averaged Hyper-2 ratio and [Ca²⁺]_i in the inner and outer region of the indicated day-6 MCF-10A acini. The acini were treated with or without 10 μ M AP-18 or 5 mM NAC (pH was adjusted to 7.4). Data shown as mean \pm SD (n = 5–13). ** $p < 0.01$ and *** $p < 0.001$ (one-way ANOVA).

(N) Representative Hyper-2 and Hyper-2 (C199S) ratio images of day-6 MCF-10A acini and averaged ratio in the inner and outer region of the acini. Scale bar 50 μ m. Data shown as mean \pm SD (n = 7–11). *** $p < 0.001$ (one-way ANOVA).

(O) Representative images of day-8 TRPA1- or vector-transduced MCF-10A acini stained with cleaved caspase-3 and percentage of acini with cleaved caspase-3-positive staining in the center. Scale bar 50 μ m. Data shown as mean \pm SEM of five independent experiments. ** $p < 0.01$ (Student's t test).

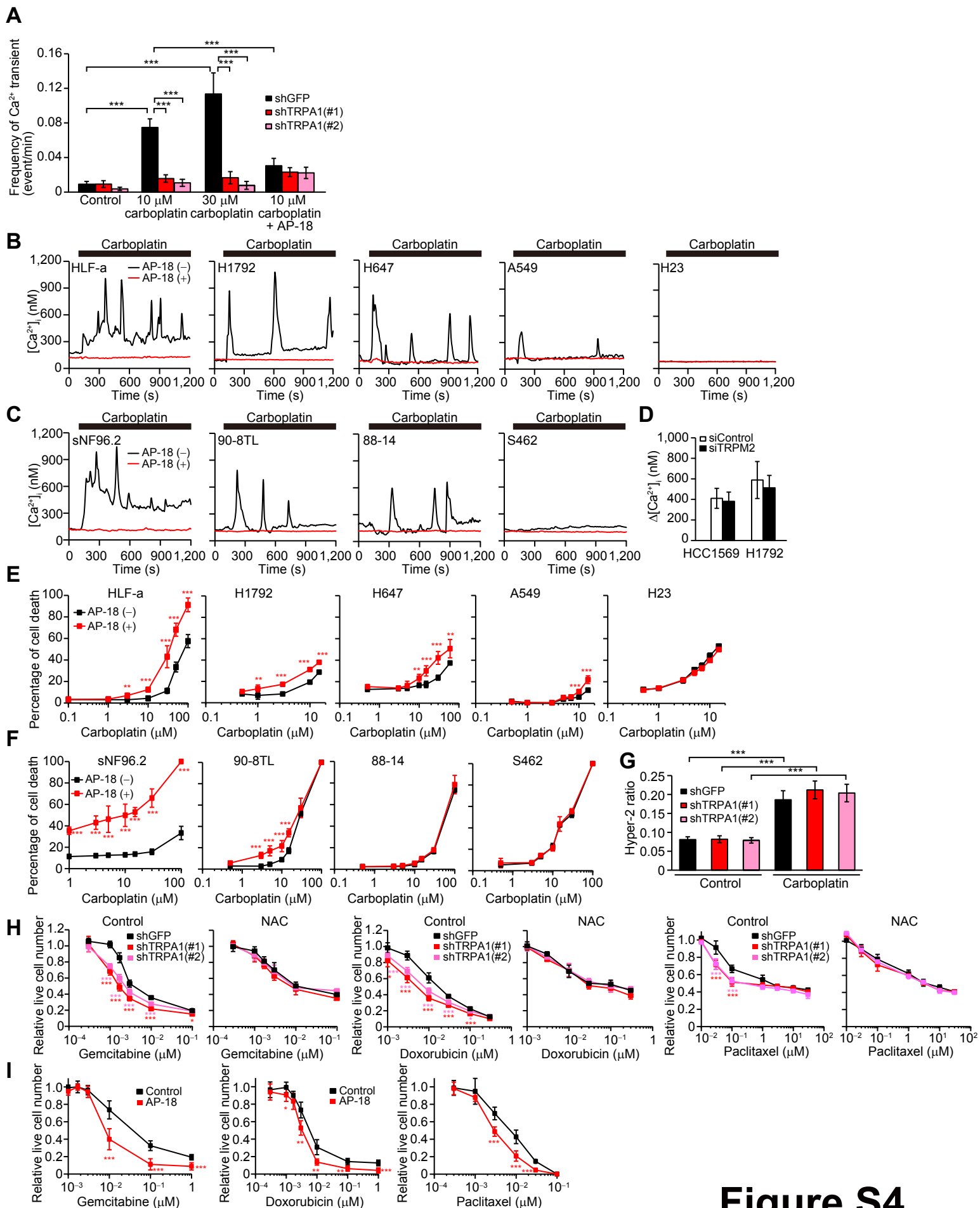


Figure S4

Figure S4. Ca²⁺ Influx through TRPA1 Suppresses Cell Death under Chemotherapy Treatment without Affecting Cellular Redox Status, Related to Figure 4.

(A) Frequency of Ca²⁺ transient ($\Delta[\text{Ca}^{2+}]_i > 200 \text{ nM}$) in HCC1569 cells transduced with shRNA against TRPA1 or GFP and treated with or without carboplatin in the presence or absence of 10 μM AP-18. Data shown as mean \pm SEM (n = 34–151). ***p < 0.001 (one-way ANOVA).

(B and C) Representative time courses of $[\text{Ca}^{2+}]_i$ changes in the indicated lung cancer (B) and MPNST cells (C) upon treatment with 10 μM carboplatin in the presence or absence of 10 μM AP-18.

(D) $\Delta[\text{Ca}^{2+}]_i$ evoked by 10 μM carboplatin in HCC1569 or H1792 cells transfected with siControl or siTRPM2. Data shown as mean \pm SEM (n = 24–31). The effect of siTRPM2 on TRPM2 mRNA expression was shown in Figure S2D.

(E and F) Percentage of cell death in the indicated lung cancer (E) and MPNST cells (F) upon treatment with carboplatin for 72 hr in the presence or absence of 10 μM AP-18. Data shown as mean \pm SD from the sum of three independent experiments performed in duplicate. **p < 0.01 and ***p < 0.001 compared to AP-18 (–) (Student's t test).

(G) Averaged Hyper-2 ratio in the indicated HCC1569 cells treated with or without 30 μM carboplatin for 48 hr. Data shown as mean \pm SEM (n = 106–233). ***p < 0.001 (one-way ANOVA).

(H) Live cell numbers relative to chemotherapy-untreated cells in the indicated HCC1569 cells treated with gemcitabine, doxorubicin, or paclitaxel in the presence or absence of 5 mM NAC (pH was adjusted to 7.4) for 72 hr. Data shown as mean \pm SD from the sum of two or three independent experiments performed in duplicate. *p < 0.05 and ***p < 0.001 compared to shGFP (Student's t test).

(I) Live cell numbers relative to chemotherapy-untreated cells in H1792 cells treated with gemcitabine, doxorubicin, or paclitaxel in the presence or absence of 10 μM AP-18 for 72 hr. Data shown as mean \pm SD from the sum of three independent experiments performed in duplicate. *p < 0.05, **p < 0.01, and ***p < 0.001 compared to vehicle control for AP-18 (Student's t test).

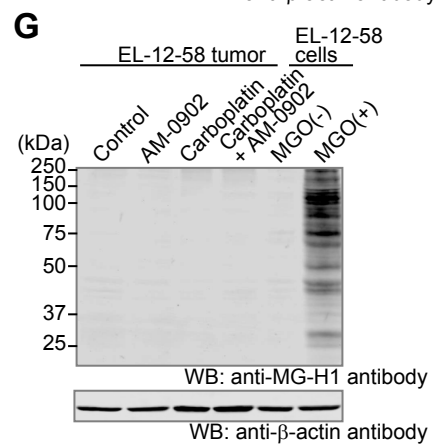
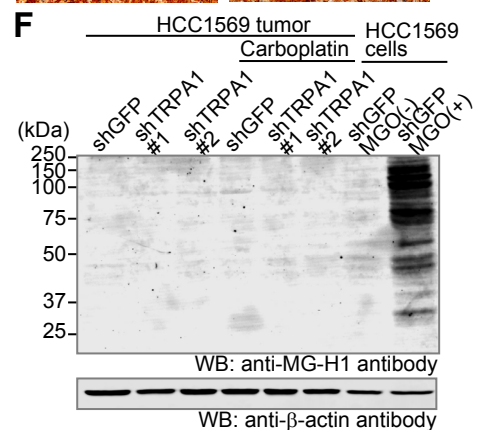
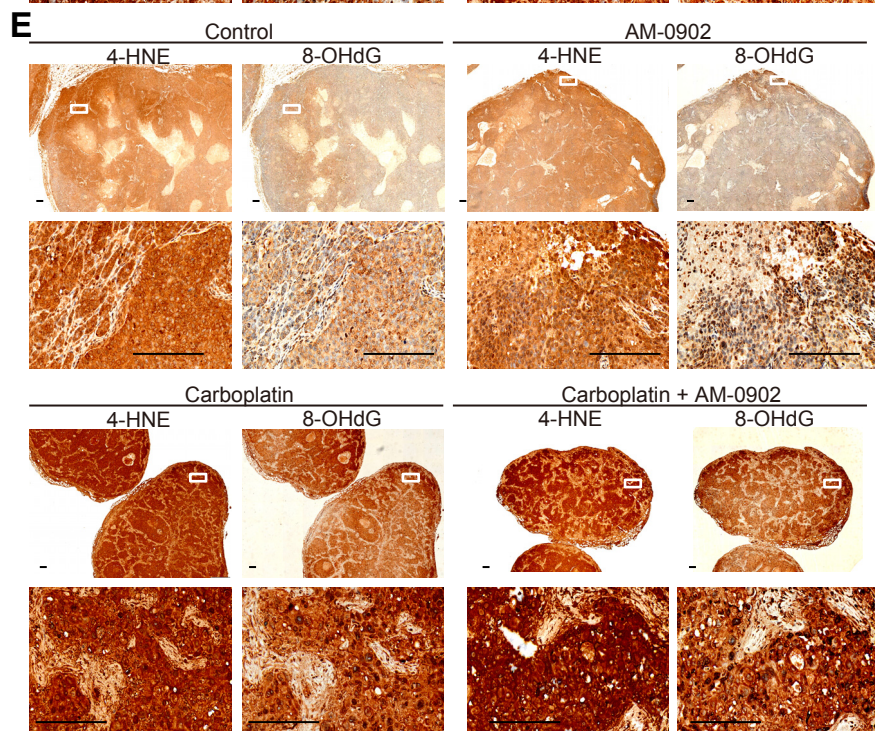
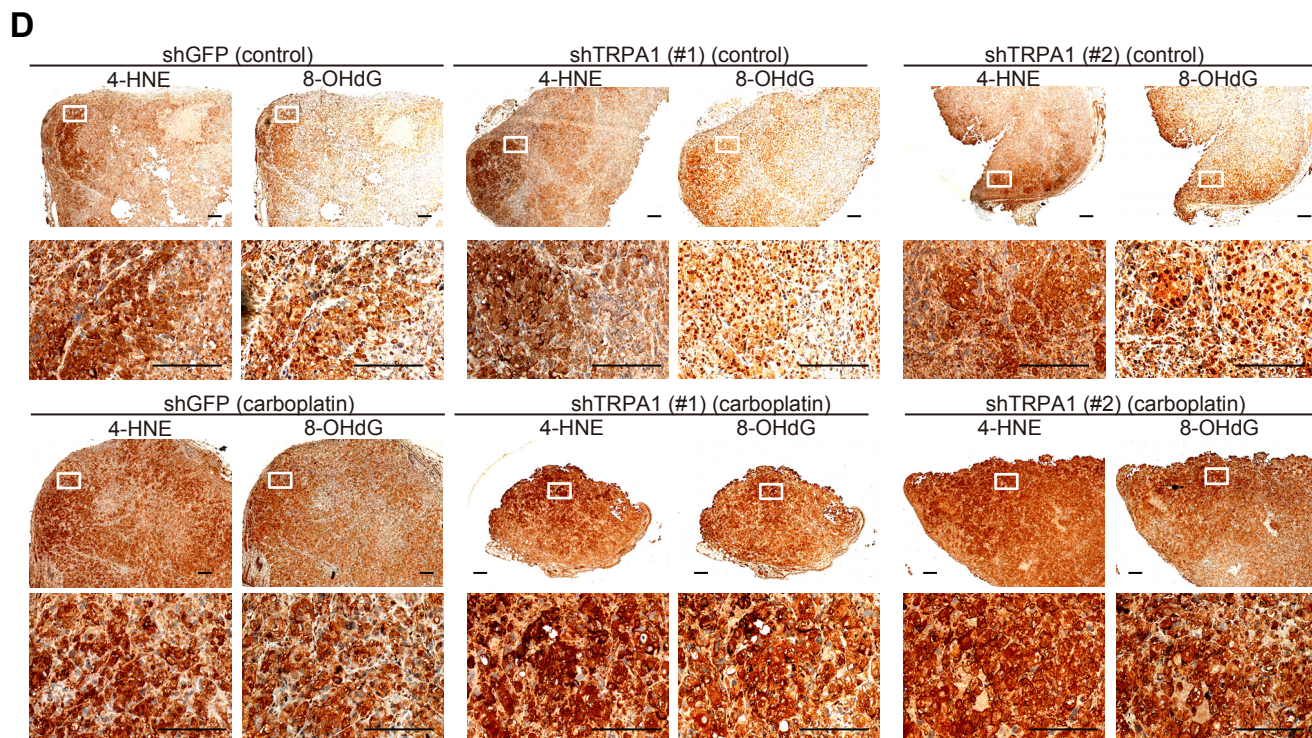
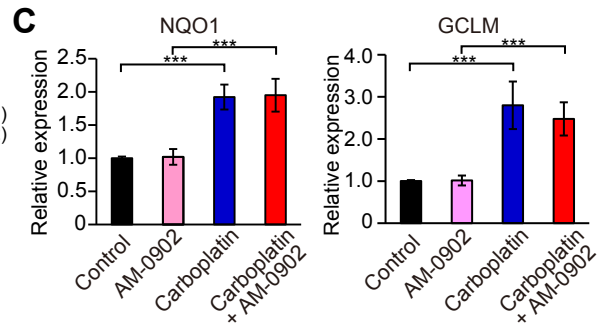
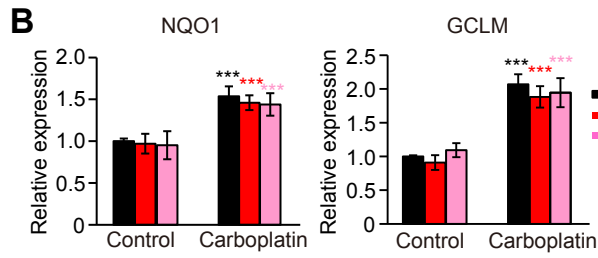
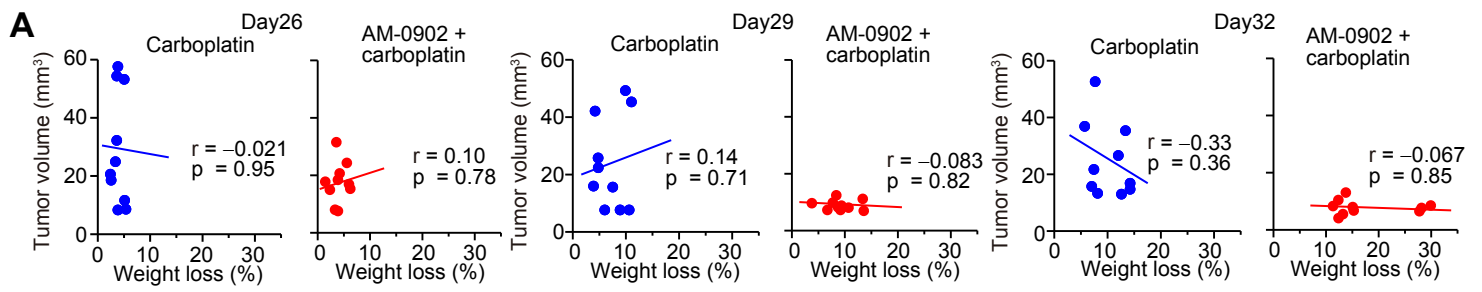


Figure S5. HCC1569 and EL-12-58 Tumors Are Exposed to Oxidative Stress but Not Dicarbonyl Stress, Related to Figure 5.

(A) Correlation of weight loss (%) with tumor volume (mm^3) in EL-12-58 xenograft tumors treated with carboplatin ($n = 10$) or AM-0902 + carboplatin ($n = 10$) at the indicated time points. Averaged weight loss: day 26, $3.94 \pm 1.02\%$ for carboplatin and $4.20 \pm 1.52\%$ for carboplatin + AM-0902; day 29, $7.01 \pm 2.80\%$ for carboplatin and $9.07 \pm 2.94\%$ for carboplatin + AM-0902; day 32, $10.3 \pm 3.36\%$ for carboplatin and $17.6 \pm 7.45\%$ for carboplatin + AM-0902. Data shown as mean \pm SD.

(B) mRNA expression of NQO1 or GCLM in the indicated HCC1569 tumors. Tumors were resected from mice in Figure 5A at the end point. Data were normalized to vehicle control. Data shown as mean \pm SD of four independent experiments. *** $p < 0.001$ compared to vehicle control (one-way ANOVA).

(C) mRNA expression of NQO1 or GCLM in the indicated EL-12-58 tumors. Tumors were resected from mice in Figure 5D at the end point. Data were normalized to vehicle control. Data shown as mean \pm SD of four independent experiments. *** $p < 0.001$ (one-way ANOVA).

(D and E) Representative images of 4-HNE or 8-OHdG IHC in HCC1569 (D) or EL-12-58 tumor sections (E). Tumors were resected from mice in Figure 5A for HCC1569 tumors or Figure 5D for EL-12-58 tumors at the end point. Enlarged views of the boxed regions shown in lower panel. Scale bar 200 μm .

(F) Methylglyoxal adducts detected by immunoblotting using anti-MG-H1 antibody in the indicated HCC1569 tumors or cells. Tumors were resected from mice in Figure 5A at the end point. Cells were treated with or without 1 mM MGO for 12 hr. Data from two independent experiments.

(G) Methylglyoxal adducts detected by immunoblotting using anti-MG-H1 antibody in the indicated EL-12-58 tumors or cells. Tumors were resected from mice in Figure 5D at the end point. Cells were treated with or without 1 mM MGO for 12 hr. Data from two independent experiments.

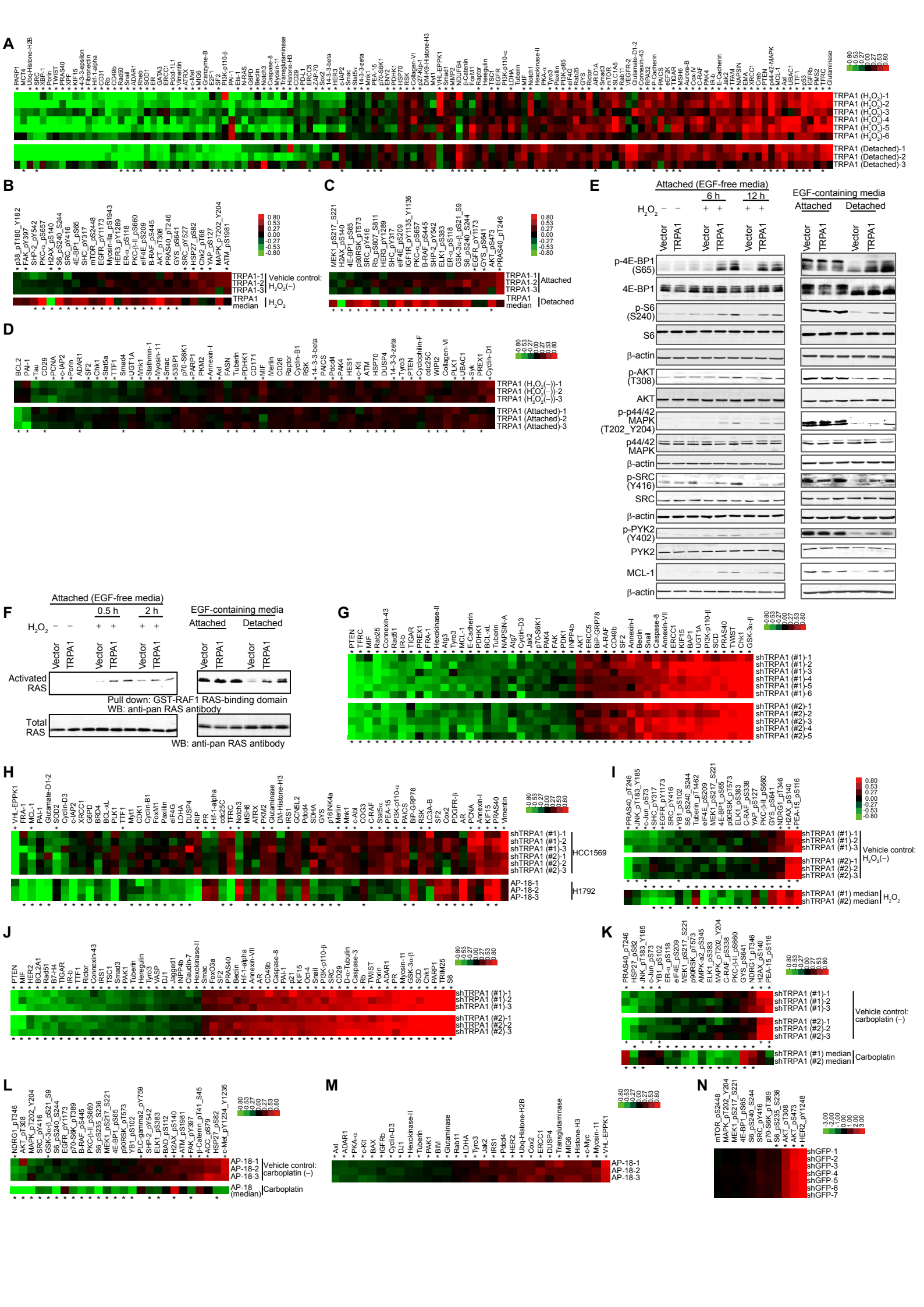


Figure S6. RPPA Analysis Reveals Signaling Pathway Alterations Induced by TRPA1 under Oxidative Stress or Carboplatin Treatment, Related to Figure 6.

(A) Heatmap of proteins whose expression was statistically significantly changed ($*p < 0.05$) between TRPA1- and vector-transduced MCF-10A cells, either in H_2O_2 treatment or in suspension (detached). Lysates of cells treated as in Figure 6A were analyzed by RPPA. Samples normalized to vector control.

(B) Heatmap of statistically significantly changed phosphorylated proteins ($*p < 0.05$) between TRPA1- and vector-transduced MCF-10A cells, either in H_2O_2 treatment or in its vehicle treatment. Cells were treated with $100 \mu M H_2O_2$ or its vehicle for 24 hr. Samples normalized to vector.

(C) Heatmap of statistically significantly changed phosphorylated proteins ($*p < 0.05$) between TRPA1- and vector-transduced MCF-10A cells, either in attachment or in detachment. Cells were cultured in adherent or non-adherent plates for 24 hr. Samples normalized to vector.

(D) Heatmap of proteins whose expression was statistically significantly changed ($*p < 0.05$) between TRPA1- and vector-transduced MCF-10A cells, either in vehicle control for H_2O_2 treatment or in attachment (control for detachment). Samples normalized to vector.

(E and F) The uncropped blots for Figure 6C (E) and 6D (F).

(G) Heatmap of proteins whose expression was statistically significantly changed ($*p < 0.05$) between shTRPA1 (#1 and #2)- and shGFP-transduced HCC1569 cells treated with $10 \mu M H_2O_2$ for 24 hr. Samples normalized to shGFP.

(H) Heatmap of proteins whose expression was statistically significantly changed ($*p < 0.05$), either between shTRPA1(#1 and #2)- and shGFP-transduced HCC1569 cells or between AP-18-treated and AP-18-untreated H1792 cells. Cells were treated with $10 \mu M$ carboplatin for 24 hr in the presence or absence of $10 \mu M$ AP-18. Samples normalized to shGFP for HCC1569 cells and AP-18 (-) for H1792 cells.

(I) Heatmap of statistically significantly changed phosphorylated proteins ($*p < 0.05$) between shTRPA1 (#1 and #2)- and shGFP-transduced HCC1569 cells, either in H_2O_2 treatment or in its vehicle treatment. Cells were treated with $10 \mu M H_2O_2$ or its vehicle for 24 hr. Samples normalized to shGFP.

(J) Heatmap of proteins whose expression was statistically significantly changed ($*p < 0.05$) between shTRPA1 (#1 and #2)- and shGFP-transduced HCC1569 cells treated with vehicle for H_2O_2 treatment. Samples normalized to shGFP.

(K) Heatmap of statistically significantly changed phosphorylated proteins ($*p < 0.05$) between shTRPA1(#1 and #2)- and shGFP-transduced HCC1569 cells, either in carboplatin treatment or in its vehicle treatment. Cells were treated with $10 \mu M$ carboplatin or its vehicle for 24 hr. Samples normalized to shGFP.

(L) Heatmap of statistically significantly changed phosphorylated proteins ($*p < 0.05$) between AP-18-treated and AP-18-untreated H1792 cells, either in carboplatin treatment or in its vehicle treatment. Cells were treated with $10 \mu M$ carboplatin or its vehicle for 24 hr in the presence or absence of $10 \mu M$ AP-18. Samples normalized to AP-18 (-).

(M) Heatmap of proteins whose expression was statistically significantly changed ($*p < 0.05$) between AP-18-treated and AP-18-untreated H1792 cells. Cells were treated with vehicle for carboplatin for 24 hr in the presence or absence of $10 \mu M$ AP-18. Samples normalized to AP-18 (-).

(N) Heatmap of RAS-ERK, AKT, and mTOR signaling proteins in shGFP-transduced HCC1569 cells treated with $10 \mu M H_2O_2$ for 24 hr. Samples normalized to TRPA1-expressing MCF-10A cells treated with $100 \mu M H_2O_2$ for 24 hr. $*p < 0.05$ compared between HCC1569 and MCF-10A cells (Student's *t* test).

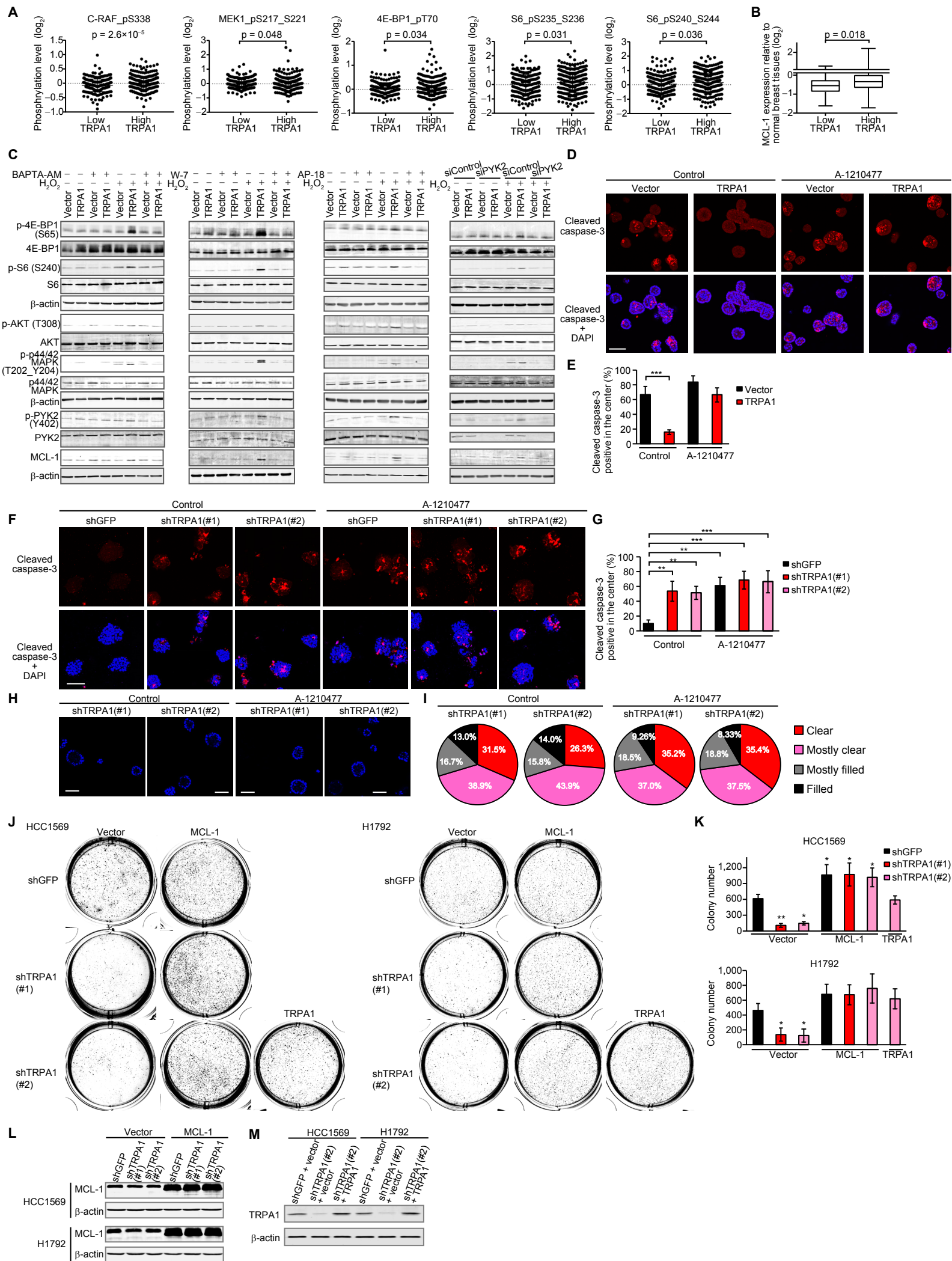


Figure S7. TRPA1 Mediates Oxidative-Stress Defense through Upregulation of Anti-Apoptotic Programs Involving MCL-1, Related to Figure 6.

(A) Phosphorylation levels of the indicated proteins in TCGA BRCA with low (percentile: < 0.4, n = 256) or high TRPA1 mRNA levels (percentile: > 0.4, n = 384). Statistical significance was determined by the Student's t test.

(B) Box plots displaying MCL-1 mRNA levels relative to normal breast tissues in TCGA BRCA with low (percentile: < 0.18, n = 104) or high TRPA1 mRNA levels (percentile: > 0.18, n = 474). Statistical significance was determined by the Student's t test.

(C) Immunoblot analysis of the effect of 10 μ M BAPTA-AM, 1 μ M W-7, 10 μ M AP-18, and siPYK2 on the indicated proteins in TRPA1- and vector-transduced MCF-10A cells treated with or without 100 μ M H₂O₂ for 12 hr in the absence of EGF in monolayer culture.

(D) Representative images of day-8 TRPA1- or vector-transduced MCF-10A acini treated with or without 3 μ M A-1210477. The spheroids were stained with cleaved caspase-3 and DAPI. Scale bar 100 μ m.

(E) Percentage of day-8 TRPA1- or vector-transduced MCF-10A acini with cleaved caspase-3 staining in the center. The spheroids were treated with or without 3 μ M A-1210477. Data shown as mean \pm SD from three independent experiments. ***p < 0.001 (one-way ANOVA).

(F) Representative images of day-10 HCC1569 spheroids treated with or without 3 μ M A-1210477. The spheroids were stained with cleaved caspase-3 and DAPI. Scale bar 100 μ m.

(G) Percentage of day-10 HCC1569 spheroids with cleaved caspase-3 staining in the center. The spheroids were treated with or without 3 μ M A-1210477. Data shown as mean \pm SD from three independent experiments. **p < 0.01 and ***p < 0.001 (one-way ANOVA).

(H) Representative images of day-13 HCC1569 transduced with shTRPA1 (#1) or shTRPA1 (#2). The spheroids were treated with or without 3 μ M A-1210477 and stained with DAPI. Scale bar 100 μ m.

(I) Pie chart of clearance levels of Day-13 HCC1569 transduced with shTRPA1 (#1) (n = 54 for control and n = 54 for A-1210477: the sum of two independent experiments) or shTRPA1 (#2) (n = 57 for control and n = 48 for A-1210477: the sum of two independent experiments). The spheroids treated with or without 3 μ M A-1210477.

(J and K) The indicated HCC1569 or H1792 cells were grown in soft agar, and after 18 days, images were taken after iodonitrotetrazolium chloride staining (J). Colony numbers are also shown (K). Data represent mean \pm SD of three independent experiments. *p < 0.05 and **p < 0.01 compared to cells transduced with both shGFP and an empty lentiviral vector (one-way ANOVA).

(L and M) Immunoblot of lysates from the indicated HCC1569 or H1792 cells transduced with an empty lentiviral vector, TRPA1, or MCL-1.

In (A) and (B), box and whiskers graphs indicate the median and the 25th and 75th percentiles, with minimum and maximum values at the extremes of the whiskers. In (C), (L), and (M), blots are representative of at least two independent experiments.

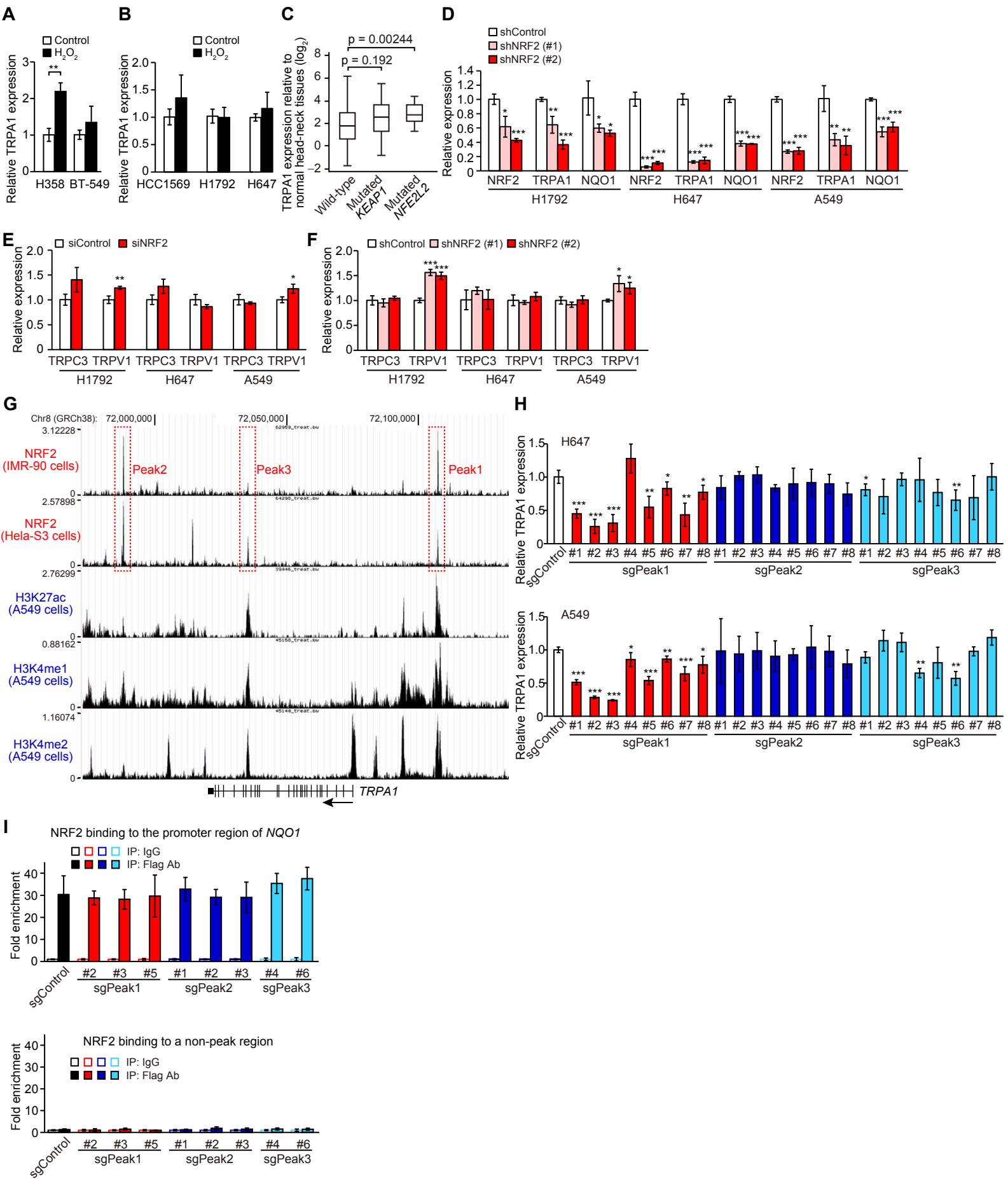


Figure S8. NRF2 Directly Induces TRPA1 Expression in Cancer Cells, Related to Figure 7.

(A) mRNA expression of TRPA1 in H358 or BT-549 cells treated with or without 10 μM H_2O_2 for 48 hr in serum-containing complete media (i.e. 10% FBS-containing media). Data were normalized to vehicle control. Data shown as mean \pm SD of three independent experiments. ** $p < 0.01$ (Student' s t test).

(B) mRNA expression of TRPA1 in HCC1569, H1792, or H647 cells treated with or without 10 μM H_2O_2 for 48 hr in serum-starved conditions (0.1% FBS). Data were normalized to vehicle control. Data shown as mean \pm SD of three independent experiments.

(C) Box plots displaying TRPA1 mRNA levels relative to normal head-neck tissues in wild-type ($n = 249$) and *KEAPI-* ($n = 13$) or *NFE2L2*-mutated HNSC ($n = 17$) based on TCGA dataset. Box and whiskers graphs indicate the median and the 25th and 75th percentiles, with minimum and maximum values at the extremes of the whiskers. Statistical significance was determined by the Student' s t test.

(D) mRNA expression of NRF2, TRPA1, and NQO1 in the indicated cancer cells transduced with doxycycline-inducible shControl or shNRF2. Cells were treated with 1 $\mu\text{g}/\text{ml}$ doxycycline for 48 hr. Data were normalized to shControl. Data shown as mean \pm SD of three independent experiments. * $p < 0.05$, ** $p < 0.01$, and *** $p < 0.001$ compared to shControl (Student' s t test).

(E) mRNA expression of TRPC3 and TRPV1 in the indicated cancer cells transfected with siControl or siNRF2. Data were normalized to siControl. Data shown as mean \pm SD of three independent experiments. * $p < 0.05$ and ** $p < 0.01$ compared to siControl (Student' s t test).

(F) mRNA expression of TRPC3 and TRPV1 in the indicated cancer cells transduced with doxycycline-inducible shControl or shNRF2. Cells were treated with 1 $\mu\text{g}/\text{ml}$ doxycycline for 48 hr. Data were normalized to shControl. Data shown as mean \pm SD of three independent experiments. * $p < 0.05$ and *** $p < 0.001$ compared to shControl (Student' s t test).

(G) Cistrome ChIP-seq data (<http://cistrome.org>) for the distribution of NRF2, histone H3K27ac, H3K4me1, and H3K36me2 are plotted around the *TRPA1* locus. The Peak1 [Chr8: 72107522–72107682 (GRCh38)], Peak2 [Chr8: 71987814–71987948 (GRCh38)], Peak3 [Chr8: 72035191–72035330 (GRCh38)].

(H) mRNA expression of TRPA1 in H647 or A549 cells transduced with Cas9 plus sgControl, sgPeak1, sgPeak2, or sgPeak3. Data were normalized to sgControl. Data shown as mean \pm SD of three independent experiments. * $p < 0.05$, ** $p < 0.01$, and *** $p < 0.001$ compared to sgControl (Student' s t test).

(I) Chromatin immunoprecipitation with Flag antibody of the fragmented chromatin containing the promoter of *NQO1* [Chr16: 69727000–69727111 (GRCh38)] or non-Peak region [Chr8: 72086158–72086422 (GRCh38)] in Flag-NRF2-overexpressing H1792 cells transduced with Cas9 plus sgControl, sgPeak1, sgPeak2, or sgPeak3. Binding was normalized to that in immunoprecipitation with IgG control. Data shown as mean \pm SD of three independent experiments.

Table S3. Expression levels of classical NRF2-induced genes in tumors with low (below median) or high TRPA1 mRNA (above median) from TCGA BRCA, LUSC, or LUAD, related to Figure 7.

	BRCA (n = 578)			LUSC (n = 501)			LUAD (n = 517)		
	mRNA level relative to normal breast tissues (log ₂)		p value (low vs high TRPA1)	mRNA level relative to normal lung tissues (log ₂)		p value (low vs high TRPA1)	mRNA level relative to normal lung tissues (log ₂)		p value (low vs high TRPA1)
	In tumors with low TRPA1	In tumors with high TRPA1		In tumors with low TRPA1	In tumors with high TRPA1		In tumors with low TRPA1	In tumors with high TRPA1	
ABCC3	-0.715	-0.448	0.0347	-0.706	-0.374	0.0371	2.47	1.90	1.08×10 ⁻⁵
GCLC	-0.323	-0.352	0.613	2.69	2.77	0.553	0.884	1.62	1.21×10 ⁻⁵
GCLM	-0.406	-0.256	0.0122	1.43	2.02	3.55×10 ⁻⁵	0.620	0.976	0.000292
GLS	-0.469	-0.295	0.0164	-0.997	-0.790	0.00204	-0.398	-0.155	0.0243
GSR	0.541	0.599	0.511	0.755	1.05	0.00660	0.652	0.676	0.801
HMOX1	0.568	0.794	0.00544	-1.08	-0.95	0.259	-0.814	-0.627	0.0286
KEAP1	0.325	0.235	0.0520	0.690	0.864	0.00624	0.114	-0.00171	0.0308
MAFG	-0.502	-0.378	0.0263	0.181	0.431	0.00105	-0.150	-0.0201	0.0257
NRF2	-0.586	-0.448	0.000414	0.685	0.511	0.0438	-0.473	-0.537	0.126
NQO1	0.422	0.461	0.738	1.41	1.89	0.0132	2.48	2.34	0.347
SLC7A11	1.239	1.69	0.000191	2.93	3.45	0.0100	2.11	2.65	0.00296
TXN	0.794	0.965	0.00270	1.26	1.52	0.0105	0.875	0.912	0.631
TXNRD1	0.130	0.290	0.0113	0.649	1.12	0.000718	0.575	1.18	3.91×10 ⁻⁵

Table S4. Primer sequences used for the construction of lentiCRISPR plasmids, related to STAR Methods.

Plasmid ID	Mutation primer sequence (5' → 3')	
	Forward primer	Reverse primer
sgPeak1 #1	caccgTGAGTCATCATTGCGGAAGT	aaacACTTCCGCAATGATGACTCAc
sgPeak1 #2	caccgACTTCCGCAATGATGACTCA	aaacTGAGTCATCATTGCGGAAGTc
sgPeak1 #3	caccgAACTTCCGCAATGATGACTC	aaacGAGTCATCATTGCGGAAGTtc
sgPeak1 #4	caccgGAAGCCCTGAGTCATCATTG	aaacCAATGATGACTCAGGGCTTCc
sgPeak1 #5	caccgAGGACCTCTATTTATTCAGC	aaacGCTGAATAAATAGAGGTCCTc
sgPeak1 #6	caccgATGGTGGAAATTTGTGTTACT	aaacAGTAACACAAATTCACCATc
sgPeak1 #7	caccgTACCATAAAGGTTTACTAAT	aaacATTAGTAAACCTTTATGGTAc
sgPeak1 #8	caccgCCACTGTATTTCAAAGCTT	aaacAAGCTTTTGAATACAGTGGc
sgPeak2 #1	caccgTAAGAGCTGAATGGTAGCAC	aaacGTGCTACCATTACAGCTCTTAc
sgPeak2 #2	caccgTTGAACTCAGGCATAGTGCT	aaacAGCACTATGCCTGAGTTCAAc
sgPeak2 #3	caccgAAGAGCTGAATGGTAGCACA	aaacTGTGCTACCATTACAGCTCTTc
sgPeak2 #4	caccgAGTGGGGCAGAAGTTTGGAC	aaacGTCCAACTTCTGCCCACTc
sgPeak2 #5	caccgGAGAGAATGACTCAGCAGAT	aaacATCTGCTGAGTCATTCTCTCc
sgPeak2 #6	caccgTTGGACTGGTAAGAGCTGAA	aaacTTCAGCTCTTACCAGTCCAAC
sgPeak2 #7	caccgGAATGGTAGCACAGGGCAGC	aaacGCTGCCCTGTGCTACCATTCC
sgPeak2 #8	caccgAGAGAGAATGACTCAGCAGA	aaacTCTGCTGAGTCATTCTCTCTc
sgPeak3 #1	caccgTTCAGGCACTGTCACACCCT	aaacAGGGTGTGACAGTGCCTGAAc
sgPeak3 #2	caccgATAGGATTTAAGACAGGTTT	aaacGAACCTGTCTTAAATCCTATc
sgPeak3 #3	caccgCTTGGCTCTGTATTATTAG	aaacCTAATAATGACAGAGCCAAGc
sgPeak3 #4	caccgACATATATAGTACTCAGCA	aaacTGCTGAGTCACTATATATGTc
sgPeak3 #5	caccgCACTAATAATGACAGAGCCA	aaacTGGCTCTGTATTATTAGTGC
sgPeak3 #6	caccgACTAATAATGACAGAGCCAA	aaacTTGGCTCTGTATTATTAGTc
sgPeak3 #7	caccgTACAAGATTCTAAAGCTGAA	aaacTTCAGCTTTAGAATCTTGTAc
sgPeak3 #8	caccgTAATAAGTCATCTTTGTCAA	aaacTTGACAAAGATGACTTATTAc

Table S5. Primer sequences used for quantitative PCR, related to STAR Methods.

Quantitative RT-PCR primers

	Primer sequence (5' → 3')	
	Forward primer	Reverse primer
TRPA1	ATCAGAAATCCACCATCGTG	TTGACTGCTCTCAACACAGTATTC
TRPC3	TTCCTGGCCATTGGCTACT	AAAAGGGCTTCGCAGAATTT
TRPV1	AGAGTCACGCTGGCAACC	CGGCAGAGACTCTCCATCAC
NRF2	GAGAGCCCAGTCTTCATTGC	TTGGCTTCTGGACTTGGAAC
NQO1	TGAAGAAGAAAGGATGGGAGGT	GGCCTTCTTTATAAGCCAGAACA
GCLM	CTCCTGCTGTGTGATGCCA	CTCGTGCGCTTGAATGTCAG
β-Actin	GACAGGATGCAGAAGGAGATC	TGCTGATCCACATCTGCTG

ChIP primers

	Primer sequence (5' → 3')	
	Forward primer	Reverse primer
Peak1 region	ATGTTTATTGCTGTGGTTTGAG	CTTCCGCAATGATGACTCAG
Peak2 region	AAGTGAGAGCCAGACAGTCC	GGAATTGAGAAGAGAAGACAGATTG
Peak3 region	CCCAGAAATAGGATTTAAGACAGG	AGGAACTTACAAGATTCTAAAGCTG
non-Peak region	GTGTACAGAATGCGGAAAAC	CCCAAAGTGCTAGGATTACAG
NQO1 promoter	AAGTGCAGAATCTGAATCTTG	AGATTCTGCTGAGTCACTGTG